IET Generation, Transmission & Distribution

Research Article

IET Journals
The Institution of Engineering and Technology

Short-term operation of a distribution company: A pseudo-dynamic tabu search-based optimisation

ISSN 1751-8687
Received on 12th May 2017
Revised 2nd March 2018
Accepted on 3rd April 2018
E-First on 22nd May 2018
doi: 10.1049/iet-gtd.2017.0731
www.ietdl.org

Marcel Chuma Cerbantes[1,2] ✉, Ricardo Fernández-Blanco[3], Miguel A. Ortega-Vazquez[4], José Roberto Sanches Mantovani[1]

[1]*Department of Electrical Engineering, Universidade Estadual Paulista, Ilha Solteira, Brazil*
[2]*Instituto Federal de Mato Grosso do Sul, Três Lagoas, Brazil*
[3]*Department of Applied Mathematics, University of Malaga, Malaga, Spain*
[4]*Grid Operations and Planning, Electric Power Research Institute, Palo Alto, USA*
✉ *E-mail: marcel.chuma@gmail.com*

Abstract: This work presents a probabilistic sequential framework for short-term operation of distribution companies (DisCos) participating in the day-ahead (DA) and real-time (RT) markets. In the proposed framework, the DisCo's operating decisions are sequentially optimised; first, in a DA operation stage, and then in RT. The DA decisions are driven by the DisCo's profit maximisation, while the DisCo aims to minimise the actions required to accommodate deviations from forecasted quantities (*i.e.* the DA decisions) in the RT operation stage. This sequential approach considers realistic voltage-sensitive loads and full *ac* power flow equations to represent the realistic network's active and reactive power injections. In addition, the operation of stationary batteries and the demand elasticity under time-varying retail prices are explicitly modelled. The two resulting models are large-scale highly non-linear non-convex mathematical problems with continuous and discrete variables. A pseudo-dynamic tabu-search-based solution algorithm is used as an alternative to conventional optimisation solvers in order to tackle the problem in an effective manner, without linearisations. Numerical results from 69- and 135-bus distribution systems illustrate the performance and the scalability of the proposed approach.

1 Introduction

Modern distribution companies (DisCos) are power system agents that simultaneously deliver electrical energy to consumers, and operate the distribution network [1]. In short-term operation, DisCos are profit-seeking entities that strive to maximise the difference between the revenue from the energy sold to consumers and the total cost of supply [2]. To attain such goal, the DisCo buys energy from the wholesale electricity market and from investor-owned distributed generators (DGs) and sells energy to consumers, while operating the network efficiently within technical limits [2, 3]. The DisCo participates in both day-ahead (DA) and real-time (RT) markets to meet the load-generation power balance in the short-term. However, trading in RT is usually risky due to the high volatility of the RT prices which may lead to monetary losses [1–4]. Therefore, the DisCo seeks to settle all its transactions on the DA operation, and use RT markets as last resort to accommodate deviations from DA quantities [4].

Within the context of a restructured electricity sector, the DisCo's operation problem has taken particular interest over the last few years, specially due to the integration of distributed energy resources (DERs) into distribution networks [5–8]. Algarni and Bhattacharya [5] propose DisCo's short-term decision models for DA and RT operations under a two-stage sequential framework. This model relies on simple deterministic formulations, thus disregarding the stochastic nature of market-clearing prices, demand, and production of renewable sources. In [6], it is proposed a sequential stochastic framework to model the DisCo's DA and RT operations. However, it is assumed that the DA market-clearing prices are known. Safdarian *et al.* [7] present a DisCo's short-term decision model including price-based demand response. The authors rely on approximated linear models to enforce active and reactive power flow constraints. Finally, a RT operation framework for a DisCo with aggregator-based demand response resources is proposed in [8]. The problem is formulated as a bilevel model to capture the rational aggregators' behaviour and then it is reformulated as a single-level mixed-integer non-linear program. The works by the authors in [5–8] also neglect the operation of network devices such as step voltage regulators (SVRs) and energy storage devices (*i.e.* stationary batteries), which drastically impact on the DisCo's short-term operation. In fact, the operating costs are lower when the operation of such network devices is properly optimised [9]. In addition, they assume a constant power load representation (*i.e.* the practical voltage-sensitive behaviour of active and reactive power loads is neglected), which may lead to suboptimal solutions.

The effect of constant power and voltage-sensitive load models in distribution planning is analysed in [10–13]. In [10], experimental results show that line losses are increased after improving the power factor and voltage profile of the substation when switching a shunt capacitor bank (SCB). Singh *et al.* [11] and Qian *et al.* [12] investigate the impact of load models on the planning of DG units. Singh *et al.* [11] demonstrate that the location and size of DG units can be significantly affected when considering practical voltage-sensitive load models. As a consequence, the results are inaccurate when a constant power load model is assumed. In [12], the authors claim that a constant power load model is no longer appropriate in networks with high penetration of DERs. In fact, the quantification of operation benefits strongly depends on the models of power flow analysis. Also, Padilha-Feltrin *et al.* [13] show that the network's Volt-VAR management is more effective when realistic voltage-sensitive load models are assumed. Therefore, voltage-sensitive load models are more accurate and better suited to represent load injections in distribution networks.

This work proposes realistic DA and RT operational planning models for a DisCo based on a probabilistic sequential framework [5, 6]. The DA model is driven by profit maximisation, while the DisCo aims to minimise the active power adjustment costs of deviations from DA forecasts in the RT model. The main contributions of this work are:

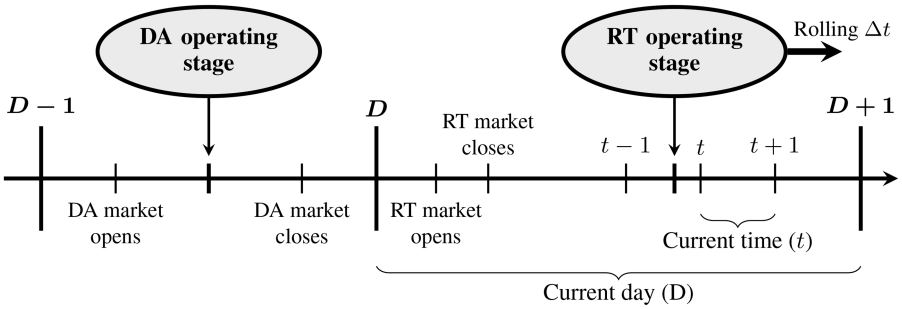

Fig. 1 *DisCo's decision timeline for current day D in the proposed sequential framework*

i. This paper proposes lifelike models for the DisCo's DA and RT operations. As customarily done in current power systems where DA and RT markets are separately run, the DisCo's DA and RT short-term operation models are implemented sequentially. An important aspect is the incorporation of realistic voltage-sensitive models for loads [11] and full *ac* power flow equations to represent the real-life nature of the network's active and reactive power injections.
ii. The proposed model includes the operation of SVRs, SCBs, and DERs, such as dispatchable/intermittent DG units and stationary batteries; and the demand elasticity as an explicit function of time-varying retail prices. The resulting models are characterised as large-scale highly non-linear non-convex programs with continuous, binary, and discrete variables due to the *ac* power flow nature, voltage-sensitive loads, and elastic demand.
iii. An effective pseudo-dynamic tabu search (TS)-based solution procedure [14] is proposed. This method is capable of handling non-continuous variables, time-coupled constraints, and the nonlinearities that characterise the problem efficiently, without resorting to linear proxies that would degrade the accuracy of the solutions. TS has proven efficiency when applied to large-scale complex planning problems in the power system literature [15–19]. Finally, a probabilistic power flow based on a fast and efficient point estimate method (PEM) [20] is used to tackle uncertainties of demand, renewable resources, and market-clearing prices.

To the best of the authors' knowledge, this is the first time that full *ac* power flow constraints with practical voltage-sensitive loads are assumed to assess the effects of Volt-VAR control provided by DERs and network devices in the DisCo's DA and RT operations. Thus, the accuracy of the DisCo's decisions in both operating stages is improved, *i.e.* a much more practical solution is obtained. One of the major obstacles in viable application of conventional optimisation solvers is the existing computational complexity associated with the non-linear terms of the resulting model plus its stochastic nature. In fact, the proposed models may not be solved by conventional optimisation techniques. Non-linear optimisation solvers would lead to intractability as the number of binary and discrete variables increases. Moreover, approximated linearisation techniques could be applied to this problem in order to yield a mixed-integer linear program. However, those techniques have two potential disadvantages: (i) they come at expense of increasing the number of constraints and variables, which may lead to intractability; and (ii) approximations unavoidably lead to inaccuracies.

The performance of the proposed approach is evaluated on a 69-bus distribution test feeder [21] and a 135-bus distribution network [22] is used for scalability purposes. In [19], the accuracy and capability of TS is successfully assessed over a conventional convex optimisation technique such as second-order conic programming.

The rest of this work is organised as follows. Section 2 addresses the problem formulation. Section 3 describes the solution approach. Section 4 analyses the numerical results. Finally, relevant conclusions are drawn in Section 5.

2 Problem formulation

The DisCo is assumed to own and operate the distribution network while behaving as a price-taker that can procure energy from the wholesale electricity market and DG units [3]. Within this context, the DisCo seeks to maximise its profits from the DA transactions. In a typical US-style forward (*i.e.* DA) electricity market, profits are given by the difference between the energy sold to customers and the purchases from the market and DG units. In RT, the objective is to minimise the adjustments required to accommodate deviations from quantities forecasted in the DA operation stage [5, 6]. Fig. 1 depicts the DisCo's decision timeline for the current day D in the proposed sequential framework. In DA, the 24 h operating decisions for the current day D are optimised a day-ahead before the DA market closes. Then, the deviations from DA decisions are adjusted in RT for each time t of the current day D based on the transactions in the RT market [23].

In the proposed model, the following assumptions are made:

- The DisCo's transactions are performed in terms of active power procurement only [3].
- DG units are investor-owned.
- Dispatchable DG units have full control of active and reactive power production.
- The production of intermittent DG units is fully injected into the network; and reactive control is possible [24].
- DG owners are paid based on the retail prices [25], *i.e.* the same price that consumers pay to the DisCo when consuming electricity.
- Time-varying retail prices are assumed the same for all types of consumers (*i.e.* residential, commercial, and industrial) [26].
- The network is equipped with the required communication and metering technology, which allows for a better integration of network devices and DERs.
- Batteries are utility-owned and can perform arbitrage.

The deterministic formulation of the proposed models is described next assuming hourly time periods.

2.1 DA operating stage

In DA operation, the DisCo needs to determine: (i) the amount of energy to be purchased from the DA market, (ii) the active power production of DG units, and (iii) the time-varying retail prices within a real-time pricing (RTP) scheme to better reflect the DA market-clearing prices; while optimising Volt-VAR control provided by DG units and network devices, such as SCBs and SVRs. These decisions are made once a day considering the uncertainties of demand, renewable resources, and DA market-clearing prices. As a consequence, deviations between the DA energy procurement and the actual energy balance may arise. It is assumed that all deviations from DA transactions are balanced in the RT operating stage. In a compact way, the DA model can be formulated as follows:

$$\max_{\Psi^{\mathrm{DA}},\, \mathcal{Z}^{\mathrm{DA}}} \quad \mathscr{B}\left(\Psi^{\mathrm{DA}}, \mathcal{Z}^{\mathrm{DA}}, \Phi^{\mathrm{DA}}\right) \tag{1}$$

subject to:

$$\Psi^{\mathrm{DA}}, \mathcal{Z}^{\mathrm{DA}}, \Phi^{\mathrm{DA}} \in \Gamma^{\mathrm{DA}}, \tag{2}$$

where $\mathcal{B}(\cdot)$ is the profit function of the DisCo in the DA operation, Ψ^{DA} is the set of control variables in the DA operation, $\mathcal{Z}^{\mathrm{DA}}$ is the set of dependent variables in the DA operation, Φ^{DA} is the set of random parameters in the DA operation, and Γ^{DA} is the feasibility set of the optimisation problem modelling the DisCo's DA operation.

The objective function (1) is driven by the maximisation of the DisCo's profit and constraint (2) represents the feasibility set of the DisCo's DA optimisation problem. The DisCo's profit can be defined as: (see (3)) where N is the set of buses; T is the set of time periods; λ_t is the retail price that consumers pay at time t for active power considering an RTP scheme; $P^{D}_{j,t}$ is the active power load at bus j and time t; G is the set of DG units; $\lambda^{\mathrm{DG}}_{g,t}$ is the price that DG unit g is paid at time t; $P^{\mathrm{DG}}_{g,t}$ is the active power produced by DG unit g at time t; S is the set of substations; $\lambda^{\mathrm{DA}}_{t}$ is the DA market-clearing price at time t; and $P^{\mathrm{DA}}_{s,t}$ is the active power purchased from external grid in the DA market at substation s and time t.

The objective function (3) comprises three terms. The first term is the total revenue for active energy sold to consumers. The second term represents the cost of the active energy produced by the DG units. Note that $\lambda^{\mathrm{DG}}_{g,t} = \lambda_t, \forall g \in G, \forall t \in T$. Finally, the third term represents the cost of active energy purchased in the DA market.

The feasibility set Γ^{DA} in (2) includes the modelling of these constraints:

- *Power flow equations:* The *ac* active and reactive power flow equations from [27] are modified to include the DA injection, production of DG units, charging/discharging of stationary batteries, and SCBs injections.
- *Voltage-sensitive load model:* A realistic voltage-sensitive load model [11] is used in this work. The active and reactive power demands depend on the active and reactive power demands at nominal voltage before response to time-varying retail prices and non-linearly with the corresponding voltage. Specific parameters are used in the voltage-sensitive load models to represent the behaviour of residential, commercial, and industrial loads and can be found in [28].
- *Demand elasticity:* The demand elasticity of consumers is modelled in terms of the time-varying retail prices, active and reactive power demands at nominal voltage before response to those prices, the price elasticity coefficients, and the daily average retail price [7, 28]. The daily average retail price can be agreed with consumers based on a contract [26] and the price elasticity coefficients can be divided into two different groups: (i) self-elasticity and (ii) cross-elasticity. Self-elasticity relates the demand response to prices associated with the same hour, whereas cross-elasticity associates the demand response to prices at different hours [29]. In this work, these coefficients are assumed to be known.
- *Retail prices:* The retail prices for active power consumption are held within minimum and maximum bounds and the daily average of the retail prices must be equal to a fixed daily average retail price, which can be agreed with consumers based on a contract [26].
- *Nodal voltage limits:* These limits ensure acceptable voltage levels at all buses. The voltage at the substation buses is held constant and equal to the nominal value, similar to the concept of slack buses used in transmission power flow calculations.
- *Substation capacity limit:* This constraint enforces the capacity limits of the substation transformers.
- *Line current limits:* These constraints enforce bounds on line current capacities.
- *Production limits of DG units:* These constraints ensure the capacity limits of DG units' active and reaction power production. In addition, the reactive power production of DG units is limited by the operating power factor limits. Finally, the power output calculation of intermittent wind turbines and PV units is done as described in [30].
- *Volt-VAR control of DG units:* The Volt control is performed by minimising the voltage magnitude mismatch so that the production of reactive power of the DG unit is based on the desired operating voltage magnitude [31]. The VAR control is based on the optimisation of the operating power factor angle within acceptable limits [31].
- *Stationary batteries:* These constraints ensure the operation of utility-owned stationary batteries. In this work, the DisCo acts as a battery aggregator to control the charging/discharging of its storage facilities [32].
- *SVRs:* The operation of type-B SVRs [33] is enforced by modelling the tap position of SVR on each line and time period.
- *SCBs*: These constraints ensure the reactive power limits of SCBs by optimising the position of switched capacitors of the SCBs.

The interested reader is referred to Appendix 1 for the detailed formulation of the constraints associated with the DisCo's DA optimisation problem.

2.2 Real-time operating stage

In RT, the DisCo seeks to minimise the cost of adjustments that are required to accommodate deviations from forecasted quantities determined in the DA stage. That is, the DisCo needs to determine the required adjustments of active power production of DG units and re-optimise Volt-VAR control provided by DG units, SCBs, and SVRs. The RT operation decisions are determined prior (*e.g.* 5 min) to time t, the current hour, in order to be applied at the beginning of time t [34], as depicted in Fig. 1.

We consider a rolling window operating planning horizon of 24 h, covering the current time t and the following $n_T - t$ time periods, as in [32]. Note that the decisions for time t and subsequent $n_T - t$ time periods are determined by considering the information on the actual realisation of the demand, renewable resources, and RT market-clearing prices. The RT approach is then formulated from t and considers all the remaining $n_T - t$ periods. In a compact way, the RT operation of the DisCo can be formulated as:

$$\min_{\Psi^{\mathrm{RT}}, \mathcal{Z}^{\mathrm{RT}}} \quad \mathcal{D}\left(\Psi^{\mathrm{RT}}, \mathcal{Z}^{\mathrm{RT}}, \Phi^{\mathrm{RT}}\right) \tag{4}$$

subject to:

$$\Psi^{\mathrm{RT}}, \mathcal{Z}^{\mathrm{RT}}, \Phi^{\mathrm{RT}} \in \Gamma^{\mathrm{RT}}, \tag{5}$$

where $\mathcal{D}(\cdot)$ is the cost function of adjustments of the DisCo in RT operation, Ψ^{RT} is the set of control variables in RT operation, $\mathcal{Z}^{\mathrm{RT}}$ is the set of dependent variables in RT operation, Φ^{RT} is the set of random parameters in RT operation, and Γ^{RT} is the feasibility set of the optimisation problem modelling the DisCo's RT operation.

The objective function (4) is driven by the minimisation of the cost of adjustments of the DisCo and constraint (5) represents the feasibility set of the DisCo's RT optimisation problem. The DisCo's deviations can be defined as:

$$\mathcal{D}(\cdot) = \sum_{g \in G} \sum_{h=0}^{n_T - t} \lambda^{\mathrm{DG}}_{g,t+h} \Delta P^{\mathrm{DG}}_{g,t+h} + \sum_{s \in S} \sum_{h=0}^{n_T - t} \lambda^{\mathrm{RT}}_{t+h} \left| P^{\mathrm{RT}}_{s,t+h} \right|, \tag{6}$$

where $\Delta P^{\mathrm{DG}}_{g,t+h}$ is the active power adjustment in RT of DG unit g at time $t+h$, which is calculated as in (7); $\lambda^{\mathrm{RT}}_{t+h}$ is the RT market-

$$\mathcal{B}(\cdot) = \sum_{j \in N} \sum_{t \in T} \lambda_t P^{D}_{j,t} - \sum_{g \in G} \sum_{t \in T} \lambda^{\mathrm{DG}}_{g,t} P^{\mathrm{DG}}_{g,t} - \sum_{s \in S} \sum_{t \in T} \lambda^{\mathrm{DA}}_{t} P^{\mathrm{DA}}_{s,t}, \tag{3}$$

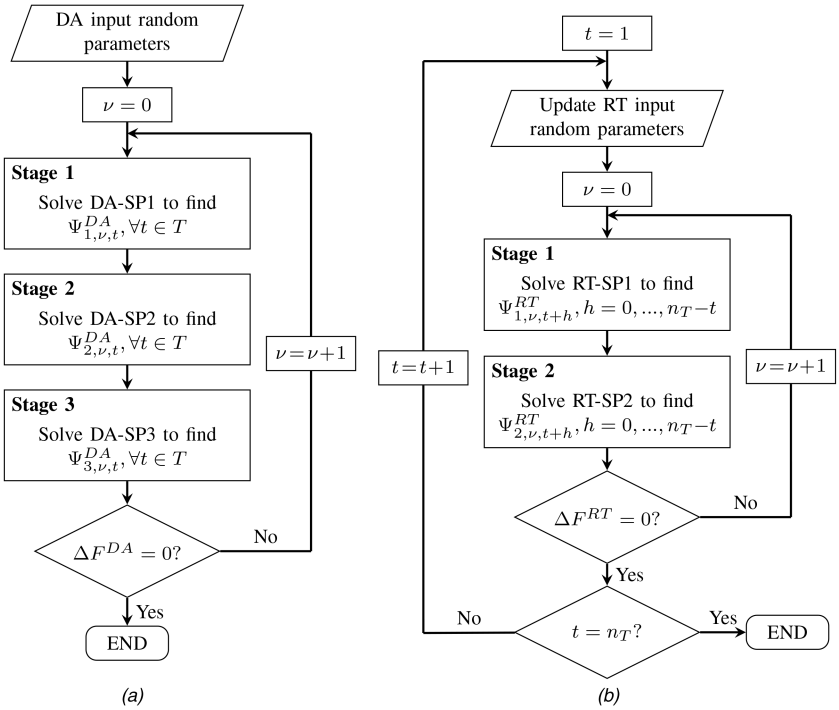

Fig. 2 *Flowcharts of the proposed TS-based solution procedures for the DisCo's short-term operation*
(a) DA operating stage, ***(b)*** RT operating stage
Note that subscripts ν and t, respectively, refer to iteration and time period and they have been added for the sake of clarity

clearing price at time $t+h$; and $P^{\mathrm{RT}}_{s,t+h}$ is the active power purchased from external grid in the RT market at substation s and time $t+h$.

$$\Delta P^{\mathrm{DG}}_{g,t+h} = \left| P^{\mathrm{DG}}_{g,t+h} - P^{\mathrm{DG}\dagger}_{g,t+h} \right|; \quad \forall g \in G, h = 0, \ldots, n_T - t, \qquad (7)$$

and where $P^{\mathrm{DG}\dagger}_{g,t+h}$ is the power purchased from DG unit g at time $t+h$ in DA; and symbol † indicates the best-known solution. It should be noted that $P^{\mathrm{DG}\dagger}_{g,t+h} = 0, \forall g \in G^{\mathrm{int}}$ (*i.e.* for the set of intermittent DG units).

The first term of the objective function (6) represents the cost of active energy produced by investor-owned DG units. The dispatchable DG units are always compensated for any deviation of the decisions taken in DA. The second term is the cost of active energy purchased in the RT market. The absolute value of $P^{\mathrm{RT}}_{s,t+h}$ in the second term reduces the DisCo's incentives for gaming in the RT market, which prevents market distortions.

The feasibility set Γ^{RT} in (5) also includes power flow equations, voltage-sensitive load models, demand elasticity of consumers to time-varying prices, nodal voltage limits, line current capacity, production limits and Volt-VAR control of DG units, operation of stationary batteries, operation of SVRs, and the reactive power limits of SCBs. Unlike constraints (2) which are defined for the whole DA time frame, the feasibility set in (5) is defined for the corresponding rolling horizon. The active power balance is also modified to consider the power purchases in the DA market and the RT injections. Finally, it is also assumed that the total active power imported from the external grid $P^{\mathrm{grid}}_{s,t+h} = P^{\mathrm{DA}\dagger}_{s,t+h} + P^{\mathrm{RT}}_{s,t+h}$.

The interested reader is referred to Appendix 2 for the detailed formulation of the constraints associated with the DisCo's RT optimisation problem.

3 Solution approach

In this section, we describe the proposed pseudo-dynamic TS-based method to solve the resulting large-scale non-linear programs with continuous and discrete variables, as described in Section 2. This proposed model includes the probabilistic approach based on a Hong's PEM [20] to handle uncertainties.

3.1 TS-based method

TS is a metaheuristic that uses a local heuristic search process to iteratively find the best-known candidate solution until a stopping criterion is met. This criterion is based on the number of iterations wherein the best-known solution remains unchanged. TS algorithm allows non-improving moves for a broader exploration of the solution space. To avoid *recurring* to previously assessed solutions and then overcoming local optima, TS uses a memory-based strategy called *tabu list* [14], which significantly improves the effectiveness of its search procedure. Its efficiency depends on two main features: (i) codification and (ii) neighbourhood. An effective decimal representation of the control variables is assumed to implement the operating decisions [16]. New candidate solutions (*i.e.* the neighbourhood) are generated at each iteration based on a combination of small changes to the control variables of the previously assessed solution. A pseudo-dynamic approach is used to create efficient neighbourhood structures, *i.e.* the neighbourhoods are designed based on the particularities of each resulting sub-problem as in [18, 19]. These features exhibit some advantages of TS over traditional metaheuristics [14]. The interested reader is referred to [14] for further details.

3.1.1 DA solution: We propose a pseudo-dynamic iterative three-stage solution process, which enforces the time-coupled constraints. The first stage is related to the interactions with the transactions on the DA operation and Volt-VAR control. The second stage addresses the operation of stationary batteries. Finally, the third stage optimises the time-varying retail prices. Then, the set of DA control variables is divided into three subsets, *i.e.* $\Psi^{\mathrm{DA}} = \left\{\Psi^{\mathrm{DA}}_1; \Psi^{\mathrm{DA}}_2; \Psi^{\mathrm{DA}}_3\right\}$, as described in Appendix 3.

Each subset comprises the DA decision control for each stage, *i.e.* DA sub-problem 1 (DA-SP1) solves for Ψ^{DA}_1, DA sub-problem 2 (DA-SP2) for Ψ^{DA}_2, and DA sub-problem 3 (DA-SP3) for Ψ^{DA}_3. At each stage, the TS algorithm is applied to solve the corresponding sub-problem based on its efficiently designed neighbourhood structure. The subsets associated with the remaining sub-problems are fixed. The resulting DA TS-based solution process is presented in Fig. 2(*a*), wherein ν is the iteration counter and ΔF^{DA} represents the difference between the fitness of the DA overall best-known solution and DA-SP1. Note that the

Table 1 Daily energy procurement (MWh)

Load profile	Total	DA market	DG units	RT market
case 1	67.03	62.80	7.01	−2.78
case 2	66.95	62.90	6.99	−2.94
case 3	66.98	62.36	7.15	−2.53
case 4	67.18	62.17	6.78	−1.77

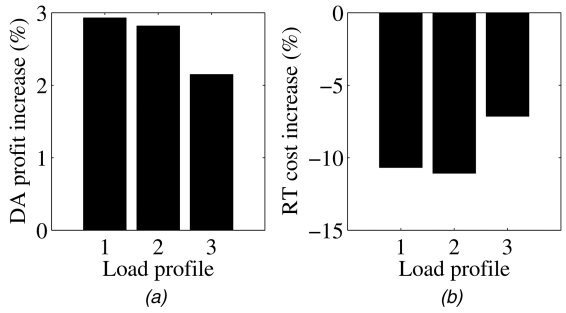

Fig. 3 *Increase of the DisCo's DA profits and RT costs for cases 1, 2, and 3 over that provided by case 4*
(a) DisCo's DA profits, ***(b)*** RT costs

fitness includes the value of the objective function and a term penalising the infeasible constraints. Thus, the fitness represents the quality measure of a candidate solution; and it is computed after solving an *ac* probabilistic power flow to determine $\mathcal{Z}^{\mathrm{DA}}$.

3.1.2 Real-time solution: A similar pseudo-dynamic iterative two-stage solution procedure is proposed to enforce the time-coupled constraints through efficient neighbourhoods. Therefore, the set of RT control variables Ψ^{RT} is divided into two subsets to represent each stage (or sub-problem): (i) the subset related to the interactions with the transactions on the RT operation and Volt-VAR control (Ψ_1^{RT}), solved in RT-SP1; and (ii) the one related with the optimisation of the operation of stationary batteries (Ψ_2^{RT}), in RT-SP2. The description of each subset can be found in Appendix 3.

Fig. 2(*b*) describes all the steps of the proposed TS-based solution procedure in RT. Note that ΔF^{RT} is calculated as the difference between the fitness of the overall best-known solution and the solution of RT-SP1 at each iteration. Again, the computation of the fitness is possible when $\mathcal{Z}^{\mathrm{RT}}$ is obtained.

3.2 $2m+1$ *PEM-based probabilistic scheme*

In order to handle the uncertainties of market-clearing prices, demand, and renewable resources considered in both DA and RT operating stages, we implement a fast and efficient $2m+1$ PEM-based probabilistic power flow algorithm [20]. This scheme provides the best performance when considering a high number of input random parameters (m). It can be seen that $2m+1$ evaluations of the objective function are required only, unlike other methods based on time-consuming Monte Carlo simulations. Therefore, the proposed approach is suitable for solving large-scale power system operational planning problems.

4 Case study

The effectiveness of the proposed approach is evaluated on a 69-bus distribution feeder [21] to examine the impacts of realistic voltage-sensitive loads in the DisCo's short-term operation. A 135-bus distribution system [22] is then used to test the scalability of the proposed method.

4.1 69-bus distribution system

The 69-bus 12.26 kV radial distribution system [21] consists of 48 buses with loads, three DG units, two SCBs, one SVR, and one substation located at bus 0′. The total system active and reactive loads are 3801.9 kW and 2694.1 kVAr. For illustrative purposes, the technical and economic data are based on that provided in [18] with the following modifications: (i) DG unit at bus 21 is a 300 kVA PV unit; (ii) the production limit of the dispatchable DG unit at bus 62 is 500 kVA; (iii) the DG's power factor limits are set to 0.8 for both leading and lagging conditions; and (iv) there are two SCBs located at buses 18 (300 kVAr fixed and two 150 kVAr switched capacitors) and 52 (600 kVAr fixed and two 300 kVAr switched capacitors). Simulation data for demand and market-clearing prices are taken from [23]; while statistical information of wind speed and solar irradiation are obtained from [35].

The proposed DA and RT operational planning models are applied to four cases of network load profiles: (i) case 1: 50% residential, 25% commercial, 25% industrial; (ii) case 2: 25% residential, 50% commercial, 25% industrial; (iii) case 3: 25% residential, 25% commercial, 50% industrial; and (iv) case 4: constant power load. The values of $\epsilon_{l,j}$, which is the percentage of load type l at bus j in the realistic voltage-sensitive load model (where $\sum_{l\in L}\epsilon_{l,j}=1$), are assumed the same at all buses [13]. Note that the first three cases are voltage-sensitive load models with non-zero values of $\alpha_{j,t}$ and $\beta_{j,t}$, which are the active and reactive exponents of load type l at bus j and time t. The values of these exponents for residential, commercial, and industrial load types can be found in [28].

4.1.1 Effect of voltage-sensitive loads: In this subsection, the effect of voltage-sensitive loads in the DisCo's short-term operation is examined. For all cases, the solutions are attained in less than 24 min. Table 1 provides the total energy procurement that the DisCo should buy to maximise profits in DA and minimise costs in RT for each load profile. This table shows also their itemised quantities, such as the energy purchased in the DA market, in the RT market, and from DG units. The energy bought from DG units includes the purchases decisions made in both the DA and RT stages. As can be seen, the DisCo's total energy procurement is always lower in the cases wherein the voltage-sensitive behaviour of loads is assumed (cases 1, 2, and 3). In fact, the maximum decrease of 0.34% is achieved in case 2 compared to the case with constant power loads (case 4). The opposite can be observed with the purchases in the DA market and from DG units, which are increased in all cases with a voltage-sensitive load profile. As a result, the amount of energy sold by the DisCo in the RT market is increased. The energy bought from DG units is greater in case 3 (5.46%), which denotes a case in which industrial loads are more important. Finally, the deviations in the RT market are increased for cases 1 (57.06%), 2 (66.10%), and 3 (42.94%).

The DisCo's DA expected profits are, respectively, \$2064.76, \$2062.54, \$2049.11, and \$2006.02 for cases 1, 2, 3, and 4; while the respective expected costs obtained by the DisCo in the RT operation are \$813.35, \$809.78, \$845.48, and \$910.53. Figs. 3(*a*) and (*b*) show the percent values of the DA profits and the RT costs for the voltage-sensitive load cases over the case with constant power loads (case 4). Fig. 3(*a*) shows that a drastic profit increase is obtained when assuming voltage-sensitive loads. The maximum increase is observed in case 1 (2.93%), in which residential load has a greater share. Conversely, the operating costs have been significantly reduced by the DisCo in the RT, as shown in Fig. 3(*b*). In fact, a significant cost reduction of 11.06% is attained in case 2, where commercial loads become more important. Therefore, the assumption of the voltage sensitiveness of load injections leads to increased profits in DA while the costs in the RT operation are lower regardless of the load profile.

The itemised economic information for cases 1, 2, and 3 over the results achieved by case 4 are presented in Figs. 4 and 5. Figs. 4(*a*)–(*c*) represent the increase in the DisCo's revenue, procurement cost, and purchase cost from DG units in the DA, whereas Figs. 5(*a*)–(*c*) represent the same information for the RT. Fig. 4(*a*) shows that the DA DisCo's revenue always increases when using a voltage-sensitive model, and it decreases in the RT operation. The largest increase in the DA revenue is achieved in case 2 (1.40%), which denotes a case in which commercial load gains more importance; whereas the DisCo's RT revenue is mostly decreased

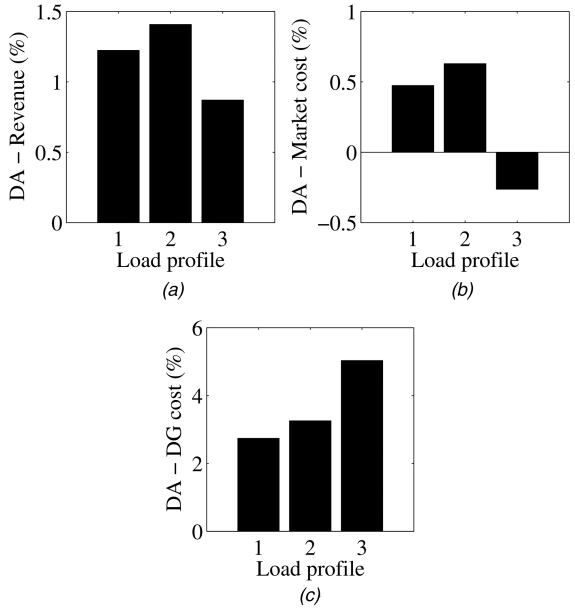

Fig. 4 *Results for the RT operation*
(a) DisCo's DA revenue, ***(b)*** Procurement cost from DA market, ***(c)*** Procurement cost from DG units in the DA
Note that the *y*-axis limits are different

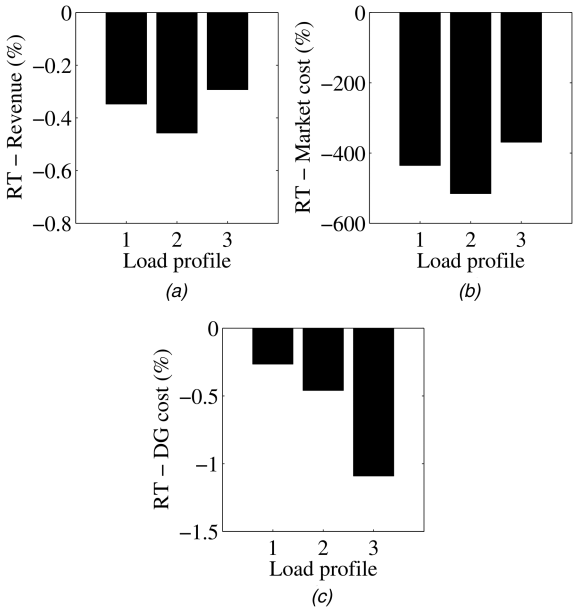

Fig. 5 *Results for the RT operation*
(a) DisCo's revenue in RT, ***(b)*** RT market procurement cost, ***(c)*** DG purchases cost in the RT operation
Note that the *y*-axis limits are different

in case 2 (0.45%). According to Fig. 4(*b*), the procurement cost from the DA market is slightly increased in cases 1 (0.47) and 2 (0.63%), and a small reduction of 0.26% is observed in case 3. However, the DisCo strives to reduce the energy bought from the RT market for the cases modelling voltage sensitiveness. In fact, the cost of deviations from RT market is strongly reduced by 515.42% in case 2 compared to case 4. A different behaviour is seen for the procurement cost from DG units when modelling voltage-sensitive loads, as shown in Fig. 4(*c*). In other words, the DisCo tends to buy more energy from DG units in the DA operation, while it is willing to slightly reduce the DG's deviation costs in the RT. It can also be observed that the DA procurement cost from DG units increases by 5.03% in case 3 and it decreases by 1.09% in the RT operation.

The cost increase of the network's active power losses for each voltage-sensitive load profile compared to the results achieved by

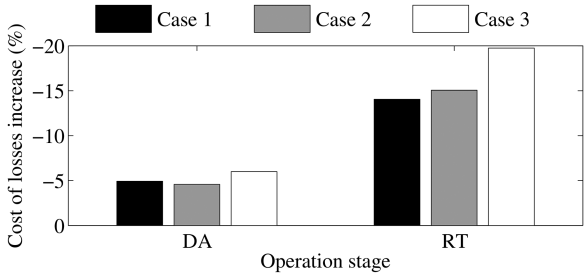

Fig. 6 *Cost increase of the network's active power losses in the DA and RT operation for cases 1, 2, and 3 over that provided by case 4*

Table 2 Profits under time-varying retail prices (TVRP) and conventional flat tariffs ($)

Load profile	DA		Diff. (%)	RT		Diff. (%)
	TVRP	Flat		TVRP	Flat	
case 1	2064.77	1912.89	7.94	2183.85	1902.06	14.82
case 2	2062.54	1898.98	9.61	2183.23	1888.57	15.60
case 3	2049.11	1878.35	9.09	2192.22	1908.10	14.89
case 4	2006.03	1840.97	8.97	2175.23	1876.65	15.91

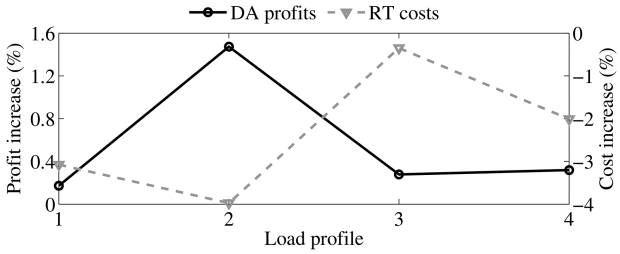

Fig. 7 *Impact of stationary batteries on the DisCo's DA profits and RT costs over the results attained without energy storage. Note that the y-axis limits are different*

the constant power load case is illustrated in Fig. 6. We can see that, regardless of the operation stage, the cost of losses is always lower when loads are represented via realistic voltage-sensitive load models. The maximum cost reduction is achieved in case 3 for both DA (5.99%) and RT (19.74%) operation stages. Thus, the consideration of realistic voltage-sensitive loads improves the operation efficiency of a distribution network.

4.1.2 Impact of pricing scheme: The type of pricing scheme applied to end-consumers plays an important role on the consumer's pattern, which in turn affects the DisCo's operation. We analyse the impact of conventional electricity rates (*i.e.* flat tariffs) compared to the time-varying pricing scheme enforced in (2). Table 2 compares the DisCo's profits in the DA and RT operation planning considering an RTP scheme and flat tariffs for cases 1, 2, 3, and 4. As expected, the profits are always higher under a time-varying pricing scheme irrespective of the load profile. The highest increase in the DisCo's DA profits is attained in case 2 (9.61%), where the importance of commercial load is more significant. On the other hand, the maximum profit increase in the RT operation (15.91%) is observed in case 4, where loads are modelled as constant power injections. Therefore, the DisCo's profitability is improved when considering time-varying retail prices.

4.1.3 Impact of energy storage systems: The five stationary batteries owned by the DisCo are used for arbitrage opportunities. It is worth mentioning that small customer-owned batteries might be aggregated and operated by the DisCo to attain maximum coordinated economic performance. To assess the impact of stationary batteries in the DisCo's short-term operation, two simulations are performed: (i) full storage capacity (500 kWh), and (ii) no storage capacity. Fig. 7 shows the impact of batteries on the DisCo's DA profits and RT costs over the results attained when no storage capacity is considered. It can be seen that the DisCo attains

Table 3 Results on computational time (s)

Load profile	69-bus		135-bus	
	DA	RT	DA	RT
case 1	1495.27	1317.22	3491.10	1733.49
case 2	1479.70	1301.49	2967.21	1784.54
case 3	1537.65	1384.69	3282.02	1629.89
case 4	970.50	1341.62	2346.27	881.27

greater profits in the DA when the batteries are utilised. However, the load profile plays an important role on how much profits the DisCo can collect. For instance, a maximum profit increase of 1.47% is achieved in case 2, when commercial loads represent a higher share. The opposite behaviour is seen in the RT operation, where the costs are always decreased by the use of batteries. Therefore, the largest cost reduction of 3.97% is also attained when commercial load is more significant (case 2).

4.2 135-bus distribution system

This subsection presents the economic results on the 135-bus, 13.8 kV, 6499.57 kW, and 2768.55 kVAr distribution test system [20] used to validate the scalability of the proposed approach. The same parameters and network devices (*i.e.* three DG units, two SCBs, one SVR, and five stationary batteries) from the previous case study are considered. In this case, DG1, DG2, and DG3 are connected to buses 87, 118, and 121. The 600 kVAr SCB is located at bus 77, and the one with 1200 kVAr is at bus 106. The SVR is installed downstream a 8 MVA substation transformer to control the voltage at bus 0. Finally, the five batteries owned by the DisCo are located at buses 21, 60, 86, 108, and 122.

The profits achieved by the DisCo in DA are \$3556.21, \$3534.82, \$3523.38, and \$3521.95 for cases 1, 2, 3, and 4; and its RT costs are \$1004.56, \$1031.96, \$1043.54, and \$1620.38, respectively. Note that the results exhibit consistency to the results achieved by the 69-bus test system. Indeed, increased profits and lower costs are always obtained when voltage-sensitive loads are assumed (cases 1, 2 and 3) compared to the case with constant power load models (case 4). The largest profit increase (0.97%) and cost reduction (38%) are achieved in case 1.

4.3 Computational performance

The proposed method was implemented in C/C++ and ran on an Intel Core CPU i7-4770 with 8 threads, 3.4 GHz, and 8 GB of RAM using Visual Studio 2013. The maximum number of iterations that the TS best-known solution should remain unchanged is set to 100.

Table 3 shows the computational time for solving DA and RT problems. The most time-consuming RT operating hours are presented. It can be seen that the computational burden increases nearly proportional to the increase in scale and complexity of the distribution network. Actually, the DA and RT problems are solved 2.30 and 1.29 times slower when the number of buses is double. Despite of that, the proposed approach is capable of solving the problem in reasonable computational times, which are acceptable within an hourly framework.

5 Conclusions

This paper presents a pseudo-dynamic TS-based probabilistic approach for short-term operation planning of a DisCo based on a sequential decision framework. This solution approach is a viable application over conventional optimisation solvers due to the high computational complexity of the proposed model. The DisCo's decisions are first optimised in a DA operating planning to maximise profits, and then its RT operation is solved to accommodate deviations while minimising costs of corrective actions. The models include realistic voltage-sensitive loads and full *ac* power flow equations to accurately represent active and reactive power injections. Numerical results show that (i) the consideration of realistic voltage-sensitive loads strongly impacts the DisCo's operation, (ii) an accurate model of voltage-sensitive loads leads to an increase of DA profits and lower RT costs, and (iii) the adoption of time-varying retail prices and batteries is also beneficial to the DisCo. Finally, the scalability of the proposed approach is successfully verified.

6 Acknowledgments

This work was supported in part by the CAPES Foundation, in part by the CNPq under Grant Agreement Number 305318/2016-0, and in part by the São Paulo Research Foundation (FAPESP) under Grant Agreement Numbers 2013/13070-7, 2014/22314-0, and 2015/21972-6.

7 References

[1] Kirschen, D., Strbac, G.: '*Fundamentals of power system economics*' (John Wiley & Sons Inc., Hoboken, NJ, USA, 2004, 1st edn.)

[2] Li, H., Li, Y., Li, Z.: 'A multiperiod energy acquisition model for a distribution company with distributed generation and interruptible load', *IEEE Trans. Power Syst.*, 2007, **22**, (2), pp. 588–596

[3] Wang, Q., Zhang, C., Wang, J., *et al.*: 'Real-time trading strategies of proactive DISCO with heterogeneous DG owners', *IEEE Trans. Smart Grid*, 2018, **9**, (3), pp. 1688–1697

[4] Stoft, S.: '*Power system economics: designing markets for electricity*' (Wiley-Interscience, New York, NY, USA, 2002, 1st edn.)

[5] Algarni, A.A.S., Bhattacharya, K.: 'A generic operations framework for DisCos in retail electricity markets', *IEEE Trans. Power Syst.*, 2009, **24**, (1), pp. 356–367

[6] Safdarian, A., Fotuhi-Firuzabad, M., Lehtonen, M.: 'A stochastic framework for short-term operation of a distribution company', *IEEE Trans. Power Syst.*, 2013, **28**, (4), pp. 4712–4721

[7] Safdarian, A., Fotuhi-Firuzabad, M., Lehtonen, M.: 'Integration of price-based demand response in DisCos' short-term decision model', *IEEE Trans. Power Syst.*, 2014, **5**, (5), pp. 2235–2245

[8] Zhang, C., Wang, Q., Wang, J., *et al.*: 'Real-time procurement strategies of a proactive distribution company with aggregator-based demand response', *IEEE Trans. Smart Grid*, 2018, **9**, (2), pp. 766–776

[9] Alnaser, S.W., Ochoa, L.F.: 'Optimal sizing and control of energy storage in wind power-rich distribution networks', *IEEE Trans. Power Syst.*, 2016, **31**, (3), pp. 2004–2013

[10] Rizy, D.T., Lawler, J.S., Patton, J.B., *et al.*: 'Measuring and analyzing the impact of voltage and capacitor control with high speed data acquisition', *IEEE Trans. Power Deliv.*, 1989, **4**, (1), pp. 704–714

[11] Singh, D., Misra, R.K., Singh, D.: 'Effect of load models in distributed generation planning', *IEEE Trans. Power Syst.*, 2007, **22**, (4), pp. 2204–2212

[12] Qian, K., Zhou, C., Allan, M., *et al.*: 'Effect of load models on assessment of energy losses in distributed generation planning', *Electr. Power Energy Syst.*, 2011, **33**, pp. 1243–1250

[13] Padilha-Feltrin, A., Rodezno, D.A.Q., Mantovani, J.R.S.: 'Volt-VAR multiobjective optimization to peak-load relief and energy efficiency in distribution networks', *IEEE Trans. Power Deliv.*, 2015, **30**, (2), pp. 618–626

[14] Lee, K.Y., El-Sharkawi, M.A.: '*Modern heuristic optimization techniques: theory and applications to power systems*' (John Wiley & Sons, Inc., Hoboken, NJ, USA, 2008, 1st edn.)

[15] Ramírez-Rosado, I.J., Domínguez-Navarro, J.A.: 'New multiobjective tabu search algorithm for fuzzy optimal planning of power distribution systems', *IEEE Trans. Power Syst.*, 2006, **21**, (1), pp. 224–233

[16] Meneses, C.A.P., Mantovani, J.R.S.: 'Improving the grid operation and reliability cost of distribution systems with dispersed generation', *IEEE Trans. Power Syst.*, 2013, **28**, (3), pp. 2485–2496

[17] Pereira Junior, B.R., Cossi, A.M., Contreras, J., *et al.*: 'Multiobjective multistage distribution system planning using tabu search', *IET Gener. Transm. Distrib.*, 2014, **8**, (1), pp. 35–45

[18] Cerbantes, M.C., Fernández-Blanco, R., Ortega-Vazquez, M.A., *et al.*: 'Optimal short-term operation of a DisCo including voltage-sensitive loads'. Proc. 19th Power Systems Computation Conf., Genoa, Italy, June 2016, pp. 1–7

[19] Cerbantes, M.C., Fernández-Blanco, R., Ortega-Vazquez, M.A., *et al.*: 'Optimal power flow with voltage-sensitive loads in distribution networks'. Proc. 2016 IEEE Power and Energy Society General Meeting, Boston, USA, July 2016, pp. 1–5

[20] Morales, J.M., Pérez-Ruiz, J.: 'Point estimate schemes to solve the probabilistics power flow', *IEEE Trans. Power Syst.*, 2007, **22**, (4), pp. 1594–1601

[21] Baran, M.E., Wu, F.F.: 'Optimal capacitor placement on radial distribution systems', *IEEE Trans. Power Deliv.*, 1989, **4**, (1), pp. 725–734

[22] Laboratory of Electrical Power System Planning National: Distribution test system – 135 buses', https://tinyurl.com/oeojrkr/, accessed 2 january 2017

[23] 'New York Independent System Operator', http://tinyurl.com/nh954ey/, accessed 17 june 2016

[24] Alam, M.J.E., Muttaqi, K.M., Sutanto, D.: 'A multi-mode control strategy for VAR support by solar PV inverters in distribution networks', *IEEE Trans. Power Syst.*, 2015, **30**, (3), pp. 1316–1326

[25] Marks, A.T., Choi, F. (Feb. 10, 2016). Renewable energy net metering tariff gets green light. Los Angeles Daily Journal. Retrieved from: https://www.milbank.com/images/content/2/3/23275/Daily-Journal-Renewable-Energy-Net-Metering-Tariff-Gets-Green-Li.pdf

[26] Zugno, M., Morales, J.M., Pinson, P., *et al.*: 'A bilevel model for electricity retailers' participation in a demand response market environment', *Energy Econ.*, 2013, **36**, pp. 182–197
[27] Gan, L., Li, N., Topcu, U., *et al.*: 'Exact convex relaxation of optimal power flow in radial networks', *IEEE Trans. Autom. Cont.*, 2015, **60**, (1), pp. 72–87
[28] IEEE Task Force on Load Representation and Dynamic Performance: 'Bibliography on load models for power flow and dynamic performance simulation', *IEEE Trans. Power Syst.*, 1995, **10**, (1), pp. 523–538
[29] Kirschen, D.S.: 'Demand-Side view of electricity market', *IEEE Trans. Power Syst.*, 2003, **18**, (2), pp. 520–527
[30] Liu, Z., Wen, F., Ledwich, G.: 'Optimal siting and sizing of distributed generators in distribution systems considering uncertainties', *IEEE Trans. Power Deliv.*, 2011, **26**, (4), pp. 2541–2551
[31] Ahmed, M.H., Bhattacharya, K., Salama, M.M.A.: 'Probabilistic distribution load flow with different wind turbine models', *IEEE Trans. Power Syst.*, 2013, **28**, (2), pp. 1540–1549
[32] Sarker, M.R., Dvorkin, Y., Ortega-Vazquez, M.A.: 'Optimal participation of an electric vehicle aggregator in day-ahead energy and reserve markets', *IEEE Trans. Power Syst.*, 2016, **31**, (5), pp. 3506–3515
[33] Kersting, W.H.: 'Distribution feeder voltage regulation control', *IEEE Trans. Ind. Appl.*, 2010, **46**, (2), pp. 620–626
[34] Conejo, A.J., Morales, J.M., Baringo, L.: 'Real-time demand response model', *IEEE Trans. Smart Grid*, 2010, **1**, (3), pp. 236–242
[35] 'National Renewable Energy Laboratory', http://www.nrel.gov/, accessed 9 July 2016

8 Appendix

8.1 Appendix 1: DA operation constraints

8.1.1 Power flow equations:

$$P^{D}_{j,t} - \sum_{g\in G_j} P^{\mathrm{DG}}_{g,t} - \sum_{s\in S_j} P^{\mathrm{DA}}_{s,t} + \sum_{b\in B_j}(c_{b,t}-d_{b,t}) = -g^{sh}_{j}|V_{j,t}|^2 - \sum_{k:\,j\to k} P_{jk,t} + \sum_{i:\,i\to j}\left(P_{ij,t} - r_{ij}|J_{ij,t}|^2\right); \quad \forall j\in N, \forall t\in T \tag{8}$$

$$Q^{D}_{j,t} - \sum_{g\in G_j} Q^{\mathrm{DG}}_{g,t} - \sum_{s\in S_j} Q^{\mathrm{grid}}_{s,t} - Q^{C}_{j,t} = -b^{sh}_{j}|V_{j,t}|^2 - \sum_{k:\,j\to k} Q_{jk,t} + \sum_{i:\,i\to j}\left(Q_{ij,t} - x_{ij}|J_{ij,t}|^2\right); \quad \forall j\in N, \forall t\in T \tag{9}$$

$$V_{j,t} = V_{i,t} - (r_{ij} + ix_{ij})J_{ij}; \quad \forall (i,j)\in E, \forall t\in T \tag{10}$$

$$J_{ij,t} = \left(\frac{P_{ij,t} + iQ_{ij,t}}{V_{i,t}}\right)^{*}; \quad \forall (i,j)\in E, \forall t\in T, \tag{11}$$

where G_j is the subset of DG units connected to bus j; S_j is the subset of substations connected to bus j; B_j is the set of batteries connected to bus j; $c_{b,t}$ and $d_{b,t}$ are the charging and discharging power rates of battery b at time t; g^{sh}_j and b^{sh}_j are the shunt conductance and susceptance at bus j, where the shunt admittance $y^{sh}_j = b^{sh}_j + ig^{sh}_j$ and i stands for the imaginary number; $V_{j,t}$ is the complex voltage at bus j and time t; E is the set of network lines; $P_{ij,t}$ and $Q_{ij,t}$ are the active and reactive power flows from bus i to j at time t; r_{ij} and x_{ij} are the resistance and reactance on line (i,j), where the line impedance $z_{ij} = r_{ij} + ix_{ij}$; $J_{ij,t}$ is the complex current from bus i to j at time t; $Q^{D}_{j,t}$ is the reactive power load at bus j and time t; $Q^{\mathrm{DG}}_{g,t}$ is the reactive power produced by DG unit g at time t; $Q^{\mathrm{grid}}_{s,t}$ is the total reactive power injection from the external grid at substation s and time t; $Q^{C}_{j,t}$ is the reactive power injection of the SCB located at bus j and time t; and the superscript $*$ stands for the conjugate operator.

In (8) and (9), the quantities $r_{ij}|J_{ij,t}|^2$ and $x_{ij}|J_{ij,t}|^2$ represent the active and reactive line losses; whereas $P_{ij,t} - r_{ij}|J_{ij,t}|^2$ and $Q_{ij,t} - x_{ij}|J_{ij,t}|^2$ represent the *receiving-end* active and reactive powers at bus j from bus i.

8.1.2 Load model:

$$P^{D}_{j,t} = P^{D0'}_{j,t}\sum_{l\in L}\epsilon_{l,j}\left|\frac{V_{j,t}}{V_n}\right|^{\alpha_{l,j,t}}; \quad \forall j\in N, \forall t\in T \tag{12}$$

$$Q^{D}_{j,t} = Q^{D0'}_{j,t}\sum_{l\in L}\epsilon_{l,j}\left|\frac{V_{j,t}}{V_n}\right|^{\beta_{l,j,t}}; \quad \forall j\in N, \forall t\in T, \tag{13}$$

where $P^{D0'}_{j,t}$ and $Q^{D0'}_{j,t}$ are the active and reactive power demands at bus j and time t at nominal voltage after response to time-varying retail prices; L is the set of load types; $\epsilon_{l,j}$ is the percentage of load type l at bus j, where $\sum_{l\in L}\epsilon_{l,j} = 1$; V_n is the network nominal or base voltage magnitude; and $\alpha_{l,j,t}$ and $\beta_{l,j,t}$ are the active and reactive exponents of load type l at bus j and time t. The values of the exponents $\alpha_{l,j,t}$ and $\beta_{l,j,t}$ for residential, commercial, and industrial load types can be found in [28]. Constraints (12) and (13) are $P^{D}_{j,t} = P^{D0'}_{j,t}$ and $Q^{D}_{j,t} = Q^{D0'}_{j,t}$ when assuming a constant power load model.

8.1.3 Demand elasticity:

$$P^{D0'}_{j,t} = P^{D0}_{j,t}\left(1 + \sum_{t'\in T} ED^{j}_{t,t'}\frac{\lambda_{t'} - \lambda^{\mathrm{avg}}}{\lambda^{\mathrm{avg}}}\right); \quad \forall j\in N, \forall t\in T \tag{14}$$

$$Q^{D0'}_{j,t} = Q^{D0}_{j,t}\left(1 + \sum_{t'\in T} ED^{j}_{t,t'}\frac{\lambda_{t'} - \lambda^{\mathrm{avg}}}{\lambda^{\mathrm{avg}}}\right); \quad \forall j\in N, \forall t\in T, \tag{15}$$

where $P^{D0}_{j,t}$ and $Q^{D0}_{j,t}$ are the active and reactive power demands at bus j and time t at nominal voltage before response to time-varying retail prices; $ED^{j}_{t,t'}$ is the price elasticity coefficient of the demand at bus j indicating how a change in price at time t' affects the demand at time t; and λ^{avg} is the daily average retail price.

8.1.4 Retail prices:

$$\underline{\lambda} \le \lambda_t \le \overline{\lambda}; \quad \forall t\in T \tag{16}$$

$$\frac{1}{n_T}\sum_{t\in T}\lambda_t = \lambda^{\mathrm{avg}}, \tag{17}$$

where $\underline{\lambda}$ and $\overline{\lambda}$ are the minimum and maximum retail prices; and n_T is the number of time periods.

8.1.5 Nodal voltage limits:

$$|V_{j,t}| = V_n; \quad \forall j\in N_s, \forall t\in T \tag{18}$$

$$\underline{V} \le |V_{j,t}| \le \overline{V}; \quad \forall j\in N\backslash N_s, \forall t\in T, \tag{19}$$

where N_s is the subset of substation buses.

8.1.6 Substation capacity limit:

$$\left(P^{\mathrm{DA}^2}_{s,t} + Q^{\mathrm{grid}^2}_{s,t}\right)^{0.5} \le \mathrm{MCS}_s; \quad \forall s\in S, \forall t\in T, \tag{20}$$

where MCS_s is the maximum capacity of substation s.

8.1.7 Line current limits:

$$|J_{ij,t}| \le \overline{J}_{ij}; \quad \forall (i,j)\in E, \forall t\in T, \tag{21}$$

where $\overline{J}_{ij}$ is the current capacity of line (i,j).

8.1.8 Production limits of DG units:

$$\underline{P}^{\mathrm{DG}}_{g} \le P^{\mathrm{DG}}_{g,t} \le \overline{P}^{\mathrm{DG}}_{g}; \quad \forall g\in G, \forall t\in T \tag{22}$$

$$\underline{Q}_g^{\mathrm{DG}} \le Q_{g,t}^{\mathrm{DG}} \le \overline{Q}_g^{\mathrm{DG}}; \quad \forall g \in G, \forall t \in T \tag{23}$$

$$\overline{S}_g^{\mathrm{DG}} \ge \left(P_{g,t}^{\mathrm{DG}^2} + Q_{g,t}^{\mathrm{DG}^2}\right)^{0.5}; \quad \forall g \in G, \forall t \in T, \tag{24}$$

where $\underline{P}_g^{\mathrm{DG}}$ and $\overline{P}_g^{\mathrm{DG}}$ are the minimum and maximum active power productions of DG unit g; $\underline{Q}_g^{\mathrm{DG}}$ and $\overline{Q}_g^{\mathrm{DG}}$ are the minimum and maximum reactive power productions of DG unit g; and $\overline{S}_g^{\mathrm{DG}}$ is the apparent power capacity of DG unit g.

In addition, the reactive power production of DG units is limited by the operating power factor limits as follows:

$$P_{g,t}^{\mathrm{DG}} \tan \underline{\delta}_g^{\mathrm{DG}} \le Q_{g,t}^{\mathrm{DG}} \le P_{g,t}^{\mathrm{DG}} \tan \overline{\delta}_g^{\mathrm{DG}}; \forall g \in G, \forall t \in T, \tag{25}$$

where $\underline{\delta}_g^{\mathrm{DG}}$ and $\overline{\delta}_g^{\mathrm{DG}}$ are the minimum (leading) and the maximum (lagging) limit of the power factor angle of DG unit g. $G = G^{\mathrm{dsp}} \cup G^{\mathrm{int}}$, where G^{dsp} and G^{int} are the sets of dispatchable and intermittent DG units.

8.1.9 Volt-VAR control of DG units: The Volt control is performed by minimising

$$\Delta\left|V_{j,t}\right| = \left|\left|V_{j,t}\right| - \left|\hat{V}_{j,t}\right|\right|; \quad \forall j \in N_g, \forall t \in T, \tag{26}$$

where $\Delta\left|V_{j,t}\right|$ is the voltage magnitude mismatch at bus j and time t; $\left|\hat{V}_{j,t}\right|$ is the desired operating voltage magnitude at bus j where the DG unit is located at time t; and N_g is the set of buses connected to DG units.

Finally, the VAR control is based on the optimisation of the operating power factor angle, within acceptable limits

$$\underline{\delta}_g^{\mathrm{DG}} \le \hat{\delta}_{g,t}^{\mathrm{DG}} \le \overline{\delta}_g^{\mathrm{DG}}; \quad \forall g \in G, \forall t \in T, \tag{27}$$

where $\hat{\delta}_{g,t}^{\mathrm{DG}}$ is the desired operational power factor angle of DG unit g at time t.

8.1.10 Stationary batteries:

$$0 \le c_{b,t} \le \gamma_{b,t} \overline{c}_b; \quad \forall b \in B, \forall t \in T \tag{28}$$

$$0 \le d_{b,t} \le (1 - \gamma_{b,t}) \overline{d}_b; \quad \forall b \in B, \forall t \in T \tag{29}$$

$$\mathrm{SoC}_{b,t} = \mathrm{SoC}_{b,t-1} + c_{b,t} \eta_b^{\mathrm{chg}} - \frac{\mathrm{d}_{b,t}}{\eta_b^{\mathrm{dsg}}}; \quad \forall b \in B, \forall t \in T \tag{30}$$

$$0 < \underline{\mathrm{SoC}}_{b,t} \le \mathrm{SoC}_{b,t} \le \overline{\mathrm{SoC}}_{b,t} < C_b; \quad \forall b \in B, \forall t \in T \tag{31}$$

$$\mathrm{SoC}_{b,n_T} = \mathrm{SoC}_{b,0}; \quad \forall b \in B, \tag{32}$$

where $\overline{c}_b$ and $\overline{d}_b$ are the maximum charging and discharging power rates of the battery b; $\gamma_{b,t} \in \{0,1\}$ prevents simultaneous charging or discharging of battery b at time t; B is the set of batteries; $\mathrm{SoC}_{b,t}$ is the energy state of charge of battery b at time t; η_b^{chg} and η_b^{dsg} are the charging and discharging efficiencies of battery b; $\underline{\mathrm{SoC}}_{b,t}$ and $\overline{\mathrm{SoC}}_{b,t}$ are the minimum and maximum allowed state of charge limits of battery b at time t; and C_b is the capacity of battery b.

8.1.11 Step voltage regulators:

$$V_{i,t} = a_{ij,t}^R V_{j,t}; \quad \forall (i,j) \in E^R, \forall t \in T \tag{33}$$

$$J_{ij,t}^2 = a_{ij,t}^R J_{ij,t}^1; \quad \forall (i,j) \in E^R, \forall t \in T \tag{34}$$

$$a_{ij,t}^R = 1 \mp \varphi_{ij}^R \, tap_{ij,t}^R; \quad \forall (i,j) \in E^R, \forall t \in T \tag{35}$$

$$-\overline{\mathrm{tap}}_{ij}^R \le \mathrm{tap}_{ij,t}^R \le \overline{\mathrm{tap}}_{ij}^R; \quad \forall (i,j) \in E^R, \forall t \in T, \tag{36}$$

where $a_{ij,t}^R$ is the regulation rate of SVR on line (i,j) at time t; E^R is the set of lines with SVRs; $J_{ij,t}^1$ and $J_{ij,t}^2$ are the line currents in the primary and secondary of SVR on line (i,j) at time t; φ_{ij}^R is the effective regulation ratio of SVR on line (i,j); and $\mathrm{tap}_{ij,t}^R$ is the tap position of SVR on line (i,j) at time t. Note that $2\overline{\mathrm{tap}}_{ij}^R$ is the total number of tap positions of SVR located on line (i,j).

8.1.12 Shunt capacitor banks:

$$Q_{j,t}^C = \underline{Q}_j^C + \kappa_{j,t}^C \, \Delta Q_j^C; \quad \forall j \in N, \forall t \in T \tag{37}$$

$$0 \le \kappa_{j,t}^C \le \overline{\kappa}_j^C; \quad \forall j \in N, \forall t \in T, \tag{38}$$

where $\overline{Q}_j^C$ is the minimum reactive power (*i.e.* the fixed capacitor) of SCB at bus j; ΔQ_j^C is the step reactive power variation (*i.e.* switched capacitors) of SCB at bus j; and $\overline{\kappa}_j^C$ is the maximum position of switched capacitors of SCB at bus j.

8.1.13 Variables in DA: The set of variables in DA are categorised into two groups: (i) the set of control variables Ψ^{DA}, and (ii) the set of dependent variables $\mathcal{Z}^{\mathrm{DA}}$

(see (39))

(see (40)) .

In this optimisation problem, the random parameters are $P_{g,t}^{\mathrm{DG}}, \forall g \in G^{\mathrm{int}}$, λ_t^{DA}, $P_{j,t}^{D0}$, and $Q_{j,t}^{D0}$.

8.2 Appendix 2: RT operation constraints

The feasibility set Γ^{RT} includes the following constraints in the RT problem:

$$\text{Constraints } (9)-(15),(18),(19),(21)-(38);\ h = 0,\ldots,n_T - t \tag{41}$$

(see (42))

(see (43)) .

The sets of variables in RT are:

(see (44))

(see (45)) .

The input random parameters are: $P_{g,t+h}^{\mathrm{DG}}, \forall g \in G^{\mathrm{int}}$, $P_{j,t+h}^{D0}$, and $Q_{j,t+h}^{D0}$; whereas $\lambda_{t+h}^{\mathrm{DA}}$ and $P_{s,t+h}^{\mathrm{DA}\dagger}$ are known quantities.

$$\Psi^{\mathrm{DA}} = \left\{ \underset{\forall g \in G^{dsp}}{P_{g,t}^{\mathrm{DG}}}; \underset{\forall j \in N_g}{\left|\hat{V}_{j,t}\right|}; \underset{\forall g \in G}{\hat{\delta}_{g,t}^{\mathrm{DG}}}; \underset{\forall b \in B}{c_{b,t}}; \underset{\forall b \in B}{d_{b,t}}; \underset{\forall b \in B}{\gamma_{b,t}}; \underset{\forall (i,j) \in E^R}{tap_{ij,t}^R}; \underset{\forall j \in N}{\kappa_{j,t}^C}; \lambda_t \right\}; \quad \forall t \in T \tag{39}$$

$$\mathcal{Z}^{\mathrm{DA}} = \left\{ \begin{array}{l} \underset{\forall s \in S}{P_{s,t}^{DA}}; \underset{\forall j \in N}{P_{j,t}^D}; \underset{\forall (i,j) \in E}{P_{ij,t}}; \underset{\forall j \in N}{V_{j,t}}; \underset{\forall (i,j) \in E}{J_{ij,t}}; \underset{\forall j \in N}{Q_{j,t}^D}; \underset{\forall g \in G}{Q_{g,t}^{\mathrm{DG}}}; \\ \underset{\forall s \in S}{Q_{s,t}^{\mathrm{grid}}}; \underset{\forall (i,j) \in E}{Q_{ij,t}}; \underset{\forall b \in B}{\mathrm{SoC}_{b,t}}; \underset{\forall (i,j) \in E^R}{a_{ij,t}^R}; \underset{\forall (i,j) \in E^R}{J_{ij,t}^{1,2}}; \underset{\forall j \in N}{Q_{j,t}^C} \end{array} \right\}; \quad \forall t \in T\,. \tag{40}$$

8.3 Appendix 3: Subsets defined for the TS-based method

The set of DA control variables (39) is divided into three subsets, *i.e.* $\Psi^{\mathrm{DA}} = \left\{\Psi_1^{\mathrm{DA}}; \Psi_2^{\mathrm{DA}}; \Psi_3^{\mathrm{DA}}\right\}$, which are defined as:

$$\Psi_1^{\mathrm{DA}} = \left\{ \underset{\forall g \in G^{dsp}}{P_{g,t}^{\mathrm{DG}}} ; \underset{\forall j \in N_g}{\left|\hat{V}_{j,t}\right|} ; \underset{\forall g \in G}{\hat{\delta}_{g,t}^{\mathrm{DG}}} ; \underset{\forall (i,j) \in E^R}{\mathrm{tap}_{ij,t}^{R}} ; \underset{\forall j \in N}{\kappa_{j,t}^{C}} \right\}; \quad \forall t \in T \tag{46}$$

$$\Psi_2^{\mathrm{DA}} = \{c_{b,t}; d_{b,t}; \gamma_{b,t}\}; \forall b \in B, \quad \forall t \in T \tag{47}$$

$$\Psi_3^{\mathrm{DA}} = \{\lambda_t\}; \quad \forall t \in T, \tag{48}$$

where Ψ_1^{DA} includes the control variables related to DA operation such as active power of dispatchable units, the magnitude of voltages in the buses connected to DG units, the desired operational power factor angles, the tap position of SVRs, and the position of switched capacitors. Ψ_2^{DA} embeds all variables related to the battery operation, *i.e.* charging and discharging power rates of the batteries and the binary variables used to prevent simultaneous charging and discharging. Finally, Ψ_3^{DA} involves the retail prices.

The set of RT control variables (44) is divided into two subsets, *i.e.* $\Psi^{\mathrm{RT}} = \left\{\Psi_1^{\mathrm{RT}}; \Psi_2^{\mathrm{RT}}\right\}$, where:

$$\Psi_1^{\mathrm{RT}} = \left\{ \underset{\forall g \in G^{dsp}}{P_{g,t+h}^{\mathrm{DG}}} ; \underset{\forall j \in N_g}{\left|\hat{V}_{j,t+h}\right|}; \underset{\forall g \in G}{\hat{\delta}_{g,t+h}^{\mathrm{DG}}}; \underset{\forall (i,j) \in E^R}{\mathrm{tap}_{ij,t+h}^{R}}; \underset{\forall j \in N}{\kappa_{j,t+h}^{C}} \right\}; \quad h = 0, \ldots, n_T - t \tag{49}$$

$$\Psi_2^{\mathrm{RT}} = \{c_{b,t+h}; d_{b,t+h}; \gamma_{b,t+h}\}; \forall b \in B, h = 0, \ldots, n_T - t, \tag{50}$$

where Ψ_1^{RT} includes the active power of dispatchable units, the magnitude of voltages in the buses connected to DG units, the desired operational power factor angles, the tap position of SVRs, and the position of switched capacitors; and Ψ_2^{RT} embeds the charging and discharging power rates of the batteries and the binary variables used to prevent simultaneous charging and discharging.

$$\begin{aligned} P_{j,t+h}^{D} - \sum_{g \in G_j} P_{g,t+h}^{\mathrm{DG}} - \sum_{s \in S_j} \left(P_{s,t+h}^{\mathrm{DA}\dagger} + P_{s,t+h}^{\mathrm{RT}}\right) + \sum_{b \in B_j} \left(c_{b,t+h} - d_{b,t+h}\right) \\ = -g_j^{sh} |V_{j,t+h}|^2 - \sum_{k:\, j \to k} P_{jk,t+h} + \sum_{i:\, i \to j} \left(P_{ij,t+h} - r_{ij} |J_{ij,t+h}|^2\right); \\ \forall j \in N, h = 0, \ldots, n_T - t \end{aligned} \tag{42}$$

$$\left[\left(P_{s,t+h}^{\mathrm{DA}\dagger} + P_{s,t+h}^{\mathrm{RT}}\right)^2 + {Q_{s,t+h}^{\mathrm{grid}}}^2\right]^{0.5} = \mathrm{MCS}_s; \quad \forall s \in S, h = 0, \ldots, n_T - t\,. \tag{43}$$

$$\Psi^{\mathrm{RT}} = \left\{ \underset{\forall g \in G^{dsp}}{P_{g,t+h}^{\mathrm{DG}}} ; \underset{\forall j \in N_g}{\left|\hat{V}_{j,t+h}\right|}; \underset{\forall g \in G}{\hat{\delta}_{g,t+h}^{\mathrm{DG}}}; \underset{\forall b \in B}{c_{b,t+h}}; \underset{\forall b \in B}{d_{b,t+h}}; \underset{\forall b \in B}{\gamma_{b,t+h}}; \underset{\forall (i,j) \in E^R}{tap_{ij,t+h}^{R}}; \underset{\forall j \in N}{\kappa_{j,t+h}^{C}} \right\}; h = 0, \ldots, n_T - t \tag{44}$$

$$\begin{aligned} \mathcal{Z}^{\mathrm{RT}} = \Bigg\{ & \underset{\forall j \in N}{P_{j,t+h}^{D}}; \underset{\forall s \in S}{P_{s,t+h}^{\mathrm{RT}}}; \underset{\forall (i,j) \in E}{P_{ij,t+h}} ; \underset{\forall j \in N}{V_{j,t+h}}; \underset{\forall (i,j) \in E}{J_{ij,t+h}} ; \underset{\forall j \in N}{Q_{j,t+h}^{D}}; \underset{\forall g \in G}{Q_{g,t+h}^{\mathrm{DG}}}; \\ & \underset{\forall s \in S}{Q_{s,t+h}^{\mathrm{grid}}}; \underset{\forall (i,j) \in E}{Q_{ij,t+h}} ; \underset{\forall b \in B}{SoC_{b,t+h}}; \underset{\forall (i,j) \in E^R}{a_{ij,t+h}^{R}} ; \underset{\forall (i,j) \in E^R}{J_{ij,t+h}^{1,2}} ; \underset{\forall j \in N}{Q_{j,t+h}^{C}} \Bigg\}; \\ & h = 0, \ldots, n_T - t, \end{aligned} \tag{45}$$